が報告されている。しかしすべての因子がどのタイミングで作用しているか明らかになっているわけではなく、少なくとも現時点ではin vitroにおいて間葉系幹細胞から腎臓まで分化させることは不可能と言わざるを得ない。そこで今回我々は外来の間葉系幹細胞を中腎管の発芽する部位に注入し、発生段階と全く同じ環境下に置くことで腎臓そのものを作り出すことが可能か検討してきた。昨年までの研究によりドナー細胞由来の尿細管上皮細胞、糸球体上皮細胞、間質細胞に分化することが確認され、さらに糸球体上皮細胞は連続性を持って尿細管上皮に移行しており、ネフロンの一部を形成していることが示された。そこで１６年度はこの事象を基に、リソゾーム代謝酵素欠損によって先天性腎障害を生じるFabry病の腎臓の一部のネフロンをwild typeに入れ替えることにより治療効果が得られるか検討した。

B．研究方法

尿管芽が発芽する直前より周囲の間葉系幹細胞はglial cell line-derived neurotrophic factor (GDNF)を発現し、そのレセプター(c-ret)を発現する尿管芽を引き込むことが後腎発生の重要なステップであることが明らかとなっているため、ヒト間葉系幹細胞に一過性にGDNFを発現させる。さらに注入した間葉系幹細胞が分化した後もレシピエントの細胞と区別できるようにレトロウイルスを用いてLacZ遺伝子を持続発現させた後、mouth pipetteを用いてE9.5で取り出したFabryマウス胎児の尿管芽発芽部位にmicroinjection行う。胎児は直ちに全胎培養器にて48時間培養し、成長した胎児より後腎原器を取り出し引き続き6日間器官培養を行った。形成された腎臓の一部が注入した正常間葉系幹細胞由来であれば、α-galactosidase A遺伝子を発現しているはずであるため、再生腎臓のα-galactosidase A酵素活性を測定し、wild type、Fabryマウスからの腎臓と比較する。さらに異常蓄積した脂質が減少しているか、抗Gb-3特異抗体を用いた免疫染色によって確認した。

C．結果

α-galactosidase 遺伝子の欠損による異常な脂質の蓄積は非常に緩除であるためFabry マウスの腎臓組織は形態的にほとんどワイルドマウスと変わりなく、また腎不全を発症する前に寿命が尽きてしまう。しかし生後6週の時点で明らかな異常脂質の蓄積が抗 Gb-3 特異抗体を用いた免疫染色にて確認されたため蓄積する異常脂質の排除を治療効果の指標とした。リレー培養法によって得られた後腎組織はその一部が注入した正常間葉系幹細胞由来であるため、α-galactosidaseの活性が上昇していることが確認された。さらにFabry マウスから得られた後腎組織は Gb-3 の異常蓄積していたが、このキメラ腎臓は蓄積した脂質がほとんど認められなかった。α-galactosidaseは正常の10%以下で脂質のクリアランスが可能であることが証明されている。さらに分泌たんぱく質であるためbystander効果があることが知られており、この遺伝子を持った細胞の周囲の細胞の脂質も代謝することが報告されているため、一部の細胞しかα-galactosidaseは陽性でないものの、その効果は拡大したものと推察される。

D．考察

今回の研究成果は閉ざされた糸球体上皮細

胞治療の糸口を発生段階に戻ってこじ開けることが可能であることを示唆するとともに、母親の骨髄を用いた出生前治療という新たな切り口の治療応用を示すものと考える。つまりFabry病のような伴性劣性遺伝形式をとる遺伝性腎疾患において胎児が罹患していることがわかった段階で、母親の骨髄細胞から間葉系幹細胞を採取しこれを用いて胎児の腎臓を母親由来の正常細胞から作り出せれば生まれてくる子供は、理論的には少なくとも腎機能傷害で透析導入になる可能性は減ると考えられる。我が子のためであればインフォームドコンセントも得やすいと考えられ、今後この分野でも研究の発展が期待される。

E. 結論

発生プロセスを用いた腎臓再生法により、外来のヒト間葉系幹細胞よりネフロンの一部を形成することに成功した。このネフロンは欠損遺伝子を供給する目的にも使用することができるため、先天性代謝疾患に伴う腎障害への治療応用に繋がると思われる。

F. 健康危険情報

本研究では、該当する情報なない。

G. 研究発表

1. 論文発表

Yokoo T, Ohashi T, Shen J-S, Sakurai K, Miyazaki Y, Utsunomiya Y, Takahashi M, Terada Y, Eto Y, Kawamura T, Osumi N, Hosoya T. Human mesenchymal stem cells in rodent whole embryo culture are reprogrammed to contribute to kidney tissues. Proceedings of the National Academy of Sciences of the United States of America 102 (9): 3296-300, 2005

2. 学会発表

1. Yokoo T, Kawamura T: Ex vivo regeneration of the murine kidney from human mesenchymal stem cells. ISN (International Society of Nephrology) Forefronts in Nephrology "Stem cell and regeneration of the kidney", January 2005, Karuizawa
2. Yokoo T, Miyazaki Y, Utsunomiya Y, Kawamura T, Hosoya T. Ex vivo regeneration of the murine kidney from human mesenchymal stem cells in cultured whole rodent embryos. The 37th Annual Meeting of the American Society of Nephrology, November 2004, St Louis

厚生科学研究費補助金（難治性疾患克服研究事業）
分担研究報告書

胎仔マイクロキメリズムの組織修復への寄与に関する検討

分担研究者　今井圓裕　大阪大学大学院・医学系研究科・病態情報内科学・助教授
研究協力者　伊藤孝仁　大阪大学大学院・医学系研究科・病態情報内科学・助手

研究要旨

胎仔マイクロキメリズムにより、出産後の母胎には胎仔由来細胞が生着しており、慢性肝障害や腎障害では、組織修復に関わることを見いだした。これは、腎臓の幹細胞研究において、臨床的にも興味深い視点からの報告である。

A. 研究目的

末期腎不全にいたる進行性腎疾患として代表的な糖尿病性腎症、IgA 腎症、高血圧性腎症などに対する治療戦略は年々進歩しているものの、依然として進行を完全に阻止することは困難であり、透析患者数の継続的な増加を見せているのが現状である。具体的には、日欧米ともに、透析患者総数は、今後も継続的に増加すると予想されている。日本透析医学会の統計によれば、平成１５年末におけるわが国の慢性透析患者数は２４万人となり、この数は、実に 10 年前の２倍以上である。過去数年来の新規透析導入患者数は、3 万人超/年のレベルであり、死亡患者数を差し引いても、毎年 1 万人以上の透析患者が増加する状況となっている。現在、30 万人の透析患者を抱える米国においても、増加率は６％前後で推移しており、2010 年までには最大 60 万人規模に到達するであろうという、National Institute of Diabetes and Digestive and Kidney Diseases (NIDDK)による予測もある。患者数の増加のみならず、患者内訳の変化も著しい。わが国において、新規導入患者の平均年齢は、昭和 61 年末で 55 歳であったが、現在では 64 歳（最高齢は 99 歳）となっており、日本人平均寿命の伸び幅を考慮しても、著明な高齢化である。さらに、透析患者では、血管合併症や感染症の合併率が非透析者に比して高いが、高齢化や透析導入の主要原因疾患である糖尿病性腎症患者の増加など、と相まって、その重症度は高まる一方である。腎疾患に関する社会的な最大の問題のひとつは、透析患者数の増加による医療費圧迫である。透析療法は、整備された工学システムと多くの医療看護スタッフを要する１人当たり年間約 500 万円以上の医療費を要する高コストの医療であり、1 万人の透析患者増加は、年間医療費が 500 億円増加することを意味する。既存透析患者の高齢化、新規導入患者層の高齢層へのシフト、合併症の増加・重症化、要介助者の著しい増加などによって透析医療自体を物理的に合理化できる要素は少なく、この視点からも新規透析導入を減らす努力が必要と考えられる。

ところで、現在(社)日本臓器移植ネットワークに登録されている腎移植希望者数は 13000 名前後であったが、例えば平成 10 年度から 13 年度にかけての脳死あるいは心停止者からの腎臓移植件数

は、例年150件前後、血縁者からの生体腎提供によるものが500-600件であり、ドナー不足が極めて深刻である。この状況は臓器提供例が多い移植先進国の米国においても同様であり、年間移植例は1万件あまりである。最近では、免疫抑制方法の進歩に伴い、ABO血液型不適合であっても良好な移植成績が得られるようになり、生体腎移植の可能性が広がっているが、健常者から臓器提供を得る生体腎移植が普遍的・抜本的な解決策となることはありえない。すなわち、現行の移植医療が最終的な解決策となりうることは、期待できないといえる。

近年、多くの分野において、機能不全に陥った臓器や欠損した組織を、再生するという試みが行われている。典型的なアプローチのひとつは、多分化能を有した幹細胞を特定系譜の方向に誘導し、それを生体内に移植して欠損した機能を補うものであり、もうひとつは、幹細胞を未分化なまま生体内局所に移植して傷害組織の修復を促進するというものである。外来投与する幹細胞の源として代表的な2つが、造血幹細胞および関葉系幹細胞を含む骨髄由来細胞と人工的に樹立されるES細胞である。また、特定の組織内に存在する内在性幹細胞は、その組織中に存在し、自己複製能と多分化能をあわせ持つ細胞である。基本的には、その組織が傷害を受けた際に修復・再生をおこなう、あるいは生理的な細胞周期のもとで、正常構築を維持するための細胞回転に関与すると考えられる。このような組織幹細胞は、発生が完了した成体組織においても、組織再生に積極的に利用できるのではないかと期待されている。組織幹細胞は、これまでは、血液系・皮膚・腸上皮などの一部の臓器のみに存在するとされてきたが、中枢神経系・骨格筋・肝臓などにも存在することが明らかとなっている。一方、実質臓器の外に存在する幹細胞としては、骨髄中の造血幹細胞や間葉系幹細胞が代表的である。特に骨髄中の幹細胞に関しては、骨・心筋・肝臓などの修復に利用可能であることが示されている。再生医療により期待できる直接的な効果として、（1）腎疾患患者は、QOLが大幅に低下する透析療法への導入を回避できる、（2）透析導入患者数の減少により、長期的に見て医療費の削減が期待できる、の2点が挙げられる。間接的にも、（3）腎不全が可逆的疾患として認識されることにより、腎疾患を有する患者ならびに家族・周辺社会の精神的・経済的負担が大幅に軽減する、（4）潜在的腎移植必要患者数の減少により、移植に伴う倫理的問題点ならびに医療費上の問題点の負担が軽減される、（5）透析施設への往復に伴う介護上の労力やコストが削減できる、などが挙げられる。より若く合併症の少ない時期に、透析導入の回避を決定づけることが可能となれば、患者の人生設計が建設的になり、社会全体の生産力を向上することも可能であろう。

我々は、現時点の医学では組織的に不可逆的な程度にまで傷害を受けた腎臓の組織に対して、積極的な働きかけを行うことによって、機能の回復を可能とする治療方法の確立を目指して研究を行なっており、平成16年度は小さいながら臨床的に意味のある知見を得た。

B．研究方法

動物：オスEGFPトランスジェニックラット（Japan SLC）とメス野生型Sprague-Dawley（SD）ラット（Japan SLC）を交配させ、出産させた母親ラットを実験に用いた。以下の、動物に関する実験プロトコールは全て、大阪大学医学部動物実験倫理委員会の承認を得ている。産後ラットSDを単独で飼育し、産直後から30日間のエタノール飲用による慢性肝障害と14日間のゲンタマイシン60 mg/kg/day皮下投与（14日間の休薬後、再び14日間皮下投与）を行った。

末梢血液の解析：30 日間の処置が終了した後、ペントバルビタール腹腔内投与による麻酔下に採血と組織摘出を行った。末梢血は、溶血後に Ficoll 分離により単核球を精製した。精製した細胞を、我々の既報に従い、FACScan (Becton Dickinson, San Jose, CA, USA)により解析した。骨髄細胞も頚骨および腓骨より採取し、解析した。末梢血液の一部は血液生化学検査に供した。組織の解析は以下のように行った。腹部大動脈より PBS ならびに 4% paraformaldehyde (PFA)/PBS で灌流を行い、肝臓および腎臓を摘出した。既報通りに凍結切片を作成し 2)、EGFP 陽性細胞の存在を検討した。肝細胞のマーカーとして、ラット抗アルブミンウサギポリクローナル抗体(Accurate Chemical and Scientific Corporation, Westbury, NY, USA)、抗ウサギ IgG 抗体(Vector Lab Inc., Burlingame, CA, USA)を用い、核を 4',6-diamidino-2-phenylindole (DAPI) (Molecular Probes, Eugene, OR, USA)にて染色した。腎臓については、抗ラミニンウサギポロクローナル抗体(Monosan, Uden, the Netherland)を用いた。

C. 結果

EGFP トランスジェニックラットは EGFP transgene をホモではなくヘテロ接合として有している。母親ラットが野生型の場合、父親 EGFP 細胞との間には 4 分の 1 の確率で、EGFP トランスジェニックラットが発生する。母親ラットは野生型であるため、産後の母体中に EGFP 陽性細胞が存在した場合には、胎仔に由来するものと考えられる。そこで、産後 30 日を経た母体末梢血液単核球分画中の EGFP 陽性細胞の有無を検討した。EGFP トランスジェニックラットでは、200 以上の EGFP 信号強度を示す細胞が 2 つのピークをもって明瞭に同定できるが、野生型ラットにはこのような細胞は存在しない。200 をカットオフ値として、産後の母体ラットを解析したところ、明らかに EGFP 陽性細胞の存在が、末梢血有核細胞 10^5 個に 1 個の頻度で確認された (図)。骨髄細胞を解析したところ、骨髄にも EGFP 陽性細胞の存在が確認された。この結果は、胎仔細胞が母体血中に侵入し、骨髄への自然生着を経て末梢血液中に細胞を供給していることを示している。

これまでの研究結果ならびに他の研究者の報告から考えて、骨髄細胞が組織に構成的に組み込まれるためには、組織が傷害を受けて損傷治癒機転が働く必要がある。そこで、産後母体を用いて慢性肝障害モデルを作成し、胎仔細胞がどのように関与するかを検討した。各ラットのエタノール平均消費量は 4 mg/kg/day 以上であり、文献的に肝傷害を誘発するに十分な摂取量であった。産後の母体ラット肝臓組織を検討したところ、EGFP 陽性細胞が肝臓組織に散在していることが確認された。EGFP 陽性細胞はアルブミン陽性であり、肝細胞であることが確認された。すなわち、胎仔細胞が母体の傷害肝組織の一部に組み込まれていることが確認された。

ゲンタマイシン投与を行った産後母体ラットは、いずれも腎機能障害を呈した。ゲンタマイシン腎症では、骨髄由来細胞が尿細管上皮に組み込まれることを既に報告している。糸球体内には EGFP 陽性細胞の存在は認められなかったが、ゲンタマイシンにより傷害を受けた尿細管においては、ラミニンで囲まれた領域内の尿細管上皮細胞に EGFP を有する細胞が確認された。顆粒状でなく、細胞質全体に EGFP シグナルが存在することから、この EGFP は、細胞自体が産生しているもので、水溶性低分子量の EGFP が糸球体濾過後にエンドサイトーシスされたものではない。傷害が持続的で組織の細胞ターンオーバーが繰り返されれば、このような細胞に由来する遺伝形質が組み込

まれる程度も増加すると予想された。

D．考察

近年の研究により、成熟年令の個体であっても、多くの組織中には幹細胞が存在していることが明らかとなり、それら幹細胞が組織の修復や生理的な組織回転に寄与している可能性が示唆されている。さらに、骨髄中には少なくとも造血系に寄与する幹細胞と間葉系幹細胞が存在することが明らかとなっている。骨髄中の幹細胞が造血系以外の系列に対して、生理的にどのような貢献を果たしているかは、いまだ未解明な部分が多いものの、少なくとも特殊な培養条件下あるいは組織環境下では、心筋、骨格筋、骨・軟骨組織、脂肪細胞などに分化することが報告されている。

妊娠母体においては、胎盤を通して胎児から母体に対して細胞の侵入が生じており、妊娠経験のある母体には少数の胎児細胞が長期間生着していると報告されている。これを microchimerism という。ヒトでは出産後 27 年以上を経ても microchimerism 状態にあった例が報告されている。胎児細胞は慢性炎症組織に観察されやすく、慢性甲状腺炎の組織や C 型慢性肝炎の組織にて、高頻度に観察されると報告されている。また、胎児細胞は母体にとって semi-allogenic であることから、Sjögren 症候群や強皮症などの自己免疫疾患の原因となっているという報告もある。母体に生着する胎児細胞には、多分化能を有した未分化細胞が含まれている可能性があり、我々は、この microchimerism と腎疾患との関係を検討した。ラットのゲンタマイシン腎症で示したような尿細管傷害はヒト疾患においても観察されることから、実際にヒトの慢性腎障害において、マイクロキメリズムにより生着した胎児細胞が、母胎の腎臓組織構築の維持に関与している可能性は極めて高い。この貢献は、おそらく、胎児細胞が骨髄に生着して、母胎の骨髄細胞と同様の性質を得ることによるものと推察される。

最近、in vitro において、複数の細胞が融合しておのおのの表現型を合わせ持つ単核の細胞が生じる現象が報告されている。胎児マイクロキメリズムによる肝臓および腎臓組織への貢献は、細胞融合による可能性が高いと考えている。この細胞融合の意義については、今後の研究が必要である。

E．結論

腎臓の修復促進・再生に関わると考えられる胎児マイクロキメリズム細胞の同定と解析を行った。

F．健康危険情報

本研究においてはラットを用いた研究であり、該当する情報はない。

G. 研究発表

1. 論文発表

1. Iwatani H, Ito T, Imai E, Matsuzaki Y, Suzuki A, Yamato M, Okabe M, Hori M. Hematopoietic and nonhematopoietic potentials of Hoechst(low)/side population cells isolated from adult rat kidney. Kidney International 65 (5): 1604-14, 2004
2. Wang Y, Iwatani H, Ito T, Horimoto N, Yamato M, Matsui I, Imai E, Hori M. Fetal cells in mother rats contribute to the remodeling of liver and kidney after injury. Biochemical and Biophysical Research Communications 325 (3): 961-7, 2004

2.学会発表

1. Yamato M, Ito T, Iwatani H, Imai E, Hori M, Ishida N. A DNA-binding protein

oscillating with the circadian rhythm orchestrates the cell cycle of rat renal epithelial cells: a novel mechanism to regulate the cell cycle. The 37th Annual Meeting of the American Society of Nephrology, November 2004, St Louis

2. Matsui I, Ito T, Imai E, Hori M. Searching for podocytes-protection system. The 37th Annual Meeting of the American Society of Nephrology, November 2004, St Louis

3. Iwatani H, Wang Y, Ito T, Yamato M, Matsui I, Imai E, Hori M. Fetal cells spontaneously engrafted in mother rats contribute to the remodeling of liver and kidney after injury. The 37th Annual Meeting of the American Society of Nephrology, November 2004, St Louis

研究成果の刊行に関する一覧表

雑誌

発表者氏名	論文タイトル名	発表誌名	巻号	ページ	出版年
Yamauchi K. Rai T. Kobayashi K. Sohara E. Suzuki T. Itoh T. Suda S. Hayama A. Sasaki S. Uchida S.	Disease-causing mutant WNK4 increases paracellular chloride permeability and phosphorylates claudins.	Proceedings of the National Academy of Sciences of the United States of America	101 (13)	4690-4694	2004
Ichihara A, Hayashi M, Kaneshiro Y, Suzuki F, Nakagawa T, Tada Y, Koura Y, Nishiyama A, Okada H, Uddin MN, Nabi AH, Ishida Y, Inagami T, Saruta T.	Inhibition of diabetic nephropathy by a decoy peptide corresponding to the "handle" region for nonproteolytic activation of prorenin.	Journal of Clinical Investigation	114 (8)	1128-35	2004
Takasato M, Osafune K, Matsumoto Y, Yoshida N, Meguro H, Aburatani H, Asashijma M, Nishinakamura R.	Identification of kidney mesenchymal genes by a combination of microarray analysis and Sall1- GFP knockin mice.	Mechanisms of Development	121 (6)	547-557	2004
Tanaka H, Terada Y, Kobayashi T, Okado T, Inoshita S, Kuwahara M, Seth A, Sato Y, S Sasaki S.	Expression and function of Ets-1 during experimental acute renal failure in rats.	Journal of the American Society of Nephrology	15 (12)	3083-3092	2004
Xie Y, Nishi S, Fukase S, Nakamura H, Chen X, Imai N, Sakatsume M, Saito A, Ueno M, Narita I, Yamamoto T, Gejyo F.	Different type and localization of CD44 on surface membrane of regenerative renal tubular epithelial cells in vivo.	American Journal of Nephrology	24 (2)	188-197	2004
Hishikawa K, Miura S, Marumo T, Yoshioka H, Mori Y, Takato T, Fujita T.	Gene expression profile of human mesenchymal stem cells during osteogenesis in three-dimensional thermoreversible gelation polymer.	Biochemical and Biophysical Research Communications	317 (4)	1103-1107	2004
Sato A, Kishida S, Tanaka T, Kikuchi A, Kodama T, Asashima M, Nishinakamura, R.	Sall1, a causative gene for Townes-Brocks syndrome, enhances the canonical Wnt signaling by localizing to heterochromatin.	Biochemical and Biophysical Research Communications	319 (1)	103-113	2004
Sato F, Narita I, Goto S, Kondo D, Saito N, Ajiro J, Saga D, Ogawa A, Kadomura M, Akiyama F, Kaneko Y, Ueno M, Sakatsume M, Gejyo F.	Transforming growth factor-beta1 gene polymorphism modifies the histological and clinical manifestations in Japanese patients with IgA nephropathy.	Tissue Antigens	64 (1)	35-42	2004

発表者氏名	論文タイトル名	発表誌名	巻号	ページ	出版年
Xie, Y. Chen, X. Nishi, S. Narita, I. Gejyo, F.	Relationship between tonsils and IgA nephropathy as well as indication of tonsillectomy.	Kidney International	65 (4)	1135-1144	2004
Miyazawa S, Hotta O, Doi N, Natori Y, Nishikawa K, Natori Y.	Role of mast cells in the development of renal fibrosis: use of mast cell-deficient rats.	Kidney International	65 (6)	2228-37	2004
Shimizu-Hirota R, Sasamura H, Kuroda M, Kobayashi E, Hayashi M, Saruta T.	Extracellular matrix glycoprotein biglycan enhances vascular smooth muscle cell proliferation and migration.	Circulation Research	94 (8)	1067-74	2004
Hishikawa K, Marumo T, Miura S, Nakanishi A, Matsuzaki Y, Shibata K, Kohike H, Komori T, Hayashi M, Nakaki T, Nakauchi H, Okano H, Fujita T.	Leukemia inhibitory factor induces multi-lineage differentiation of adult stem-like cells in kidney via kidney-specific cadherin 16.	Biochemical and Biophysical Research Communications	328 (1)	288-291	2005
Alchi B, Nishi S, Kondo D, Kaneko Y, Matsuki A, Imai N, Ueno M, Iguchi S, Sakatsume M, Narita I, Yamamoto T Gejyo F.	Osteopontin expression in acute renal allograft rejection.	Kidney International	67 (3)	886-96	2005
Ohtsubo S, Iida A, Nitta K, Tanaka T, Yamada R, Ohnishi Y, Maeda S, Tsunoda T, Takei T, Obara W, Akiyama F, Ito K, Honda K, Uchida K, Tsuchiya K, Yumura W, Ujiie T, Nagane Y, Miyano S, Suzuki Y, Narita I, Gejyo F, Fujioka T, Nihei H, Nakamura Y.	Association of a single-nucleotide polymorphism in the immunoglobulin mu-binding protein 2 gene with immunoglobulin A nephropathy.	Journal of Human Genetics	50 (1)	30-35	2005
Uchimura H, Marumo T, Takase O, Kawachi H, Shimizu F, Hayashi M, Saruta T, Hishikawa K, Fujita T.	Intrarenal injection of bone marrow-derived angiogenic cells reduces endothelial injury and mesangial cell activation in experimental glomerulonephritis.	Journal of the American Society of Nephrology	in press		2005
Yokoo T, Ohashi T, Shen JS, Sakurai K, Miyazaki Y, Utsunomiya Y, Takahashi M, Terada Y, Eto Y, Kawamura T, Osumi N, Hosoya T.	Human mesenchymal stem cells in rodent whole-embryo culture are reprogrammed to contribute to kidney tissues.	Proceedings of the National Academy of Sciences of the United States of America	102 (9)	3296-300	2005

発表者氏名	論文タイトル名	発表誌名	巻号	ページ	出版年
Iwatani H, Ito T, Imai E, Matsuzaki Y, Suzuki A, Yamato M, Okabe M, Hori M.	Hematopoietic and nonhematopoietic potentials of Hoechst(low)/side population cells isolated from adult rat kidney.	Kidney International	65 (5)	1604-14	2004
Wang Y, Iwatani H, Ito T, Horimoto N, Yamato M, Matsui I, Imai E, Hori M.	Fetal cells in mother rats contribute to the remodeling of liver and kidney after injury.	Biochemical and Biophysical Research Communications	325 (3)	961-7	2004

Disease-causing mutant WNK4 increases paracellular chloride permeability and phosphorylates claudins

Kozue Yamauchi, Tatemitsu Rai, Katsuki Kobayashi, Eisei Sohara, Tatsunori Suzuki, Tomohiro Itoh, Shin Suda, Atsushi Hayama, Sei Sasaki, and Shinichi Uchida*

Department of Nephrology, Graduate School, Tokyo Medical and Dental University, 1-5-45 Yushima Bunkyo, Tokyo 113-8519, Japan

Edited by Maurice B. Burg, National Institutes of Health, Bethesda, MD, and approved January 28, 2004 (received for review October 26, 2003)

Mutations in the WNK4 gene cause pseudohypoaldosteronism type II (PHAII), an autosomal-dominant disorder of hyperkalemia and hypertension. The target molecules of this putative kinase and the molecular mechanisms by which the mutations cause the phenotypes are currently unknown. Although recent reports found that expression of WNK4 in *Xenopus* oocytes causes inhibition of the thiazide-sensitive NaCl cotransporter and the renal K channel ROMK, there may be additional targets of WNK4. For example, an increase in paracellular chloride permeability has been postulated to be a mediator of PHAII pathogenesis, a possibility supported by the localization of WNK4 at tight junctions *in vivo*. To determine the validity of this hypothesis, we measured transepithelial Na and Cl permeability in Madin–Darby canine kidney II cells stably expressing wild-type or a pathogenic mutant of WNK4. We found that transepithelial paracellular Cl permeability was increased in cells expressing a disease-causing mutant WNK4 (D564A) but that Na permeability was decreased slightly. Furthermore, WNK4 bound and phosphorylated claudins 1–4, major tight-junction membrane proteins known to be involved in the regulation of paracellular ion permeability. The increases in phosphorylation of claudins were greater in cells expressing the mutant WNK4 than in cells expressing wild-type protein. These results clearly indicate that the pathogenic WNK4 mutant possesses a gain-of-function activity and that the claudins may be important molecular targets of WNK4 kinase. The increased paracellular "chloride shunt" caused by the mutant WNK4 could be the pathogenic mechanism of PHAII.

Pseudohypoaldosteronism type II (PHAII) [OMIM (online Mendelian inheritance in man) database no. 145260] is a rare Mendelian form of hypertension. Recently, mutations in two homologous protein kinase genes, *WNK1* and *WNK4*, were linked to PHAII by positional cloning (1). Determination of the pathogenesis of rare Mendelian forms of high blood pressure may provide important clues to the pathways underlying more common hypertension, termed "essential" hypertension, and may help identify new therapeutic targets. PHAII-causing mutations in the *WNK1* gene are large deletions in the first intron that appear to increase WNK1 expression. On the other hand, mutations in the *WNK4* gene are missense mutations that cluster within a span of four amino acids distal to the first putative coil domain (1). However, the consequence of these missense mutations for WNK4 function is poorly understood.

WNK1 and WNK4 are expressed in the distal nephron, suggesting that both kinases are involved in a previously unrecognized signaling pathway that regulates NaCl resorption in the distal nephron. However, the upstream regulators and the downstream molecular targets of these kinases are currently unknown. Based on clinical observations, two hypotheses have been proposed to explain the pathogenesis of PHAII. First, the mutations may cause an increase in distal nephron chloride permeability, also known as a "chloride shunt" (2). This increased chloride permeability would increase Na resorption and depolarize the transepithelial voltage, leading to hypertension and hyperkalemia, respectively. The second possibility is that the mutations increase the activity of the Na-dependent Cl cotransporter (TSC). This possibility is supported by the fact that PHAII can be treated with thiazide diuretics (3).

Recently, inhibition of TSC activity by wild-type WNK4, but not by the disease-causing mutant, was demonstrated in *Xenopus* oocytes (4, 5). Very recently, inhibition of the surface expression of ROMK channel by wild-type WNK4 was also reported. Interestingly, the disease-causing mutant further inhibited the surface expression of ROMK (6). However, these functional assays were performed only in *Xenopus* oocytes, and, to our knowledge, there have not been reports on the substrates of WNK4. TSC and ROMK are localized in the apical plasma membranes of distal nephron segments (7–9), whereas WNK4 is present in the tight-junction complexes in the cortical collecting ducts as well as in DCT (1). This finding suggests that there may be other molecular targets of WNK4, possibly including tight-junction proteins.

In this study, we first examined whether the expression of the wild-type or the disease-causing mutant WNK4 affects transepithelial paracellular ion permeability. To this end, we generated stable Madin–Darby canine kidney II (MDCK II) cell lines expressing the wild-type and one of the human disease-causing mutants (D564A) of WNK4 by using a tetracycline-inducible system. We found that transepithelial paracellular Cl permeability was increased in cells expressing the mutant WNK4. Accordingly, we searched for the downstream molecular target of WNK4 in tight-junction proteins.

Materials and Methods

Generation of WNK4-Expressing Cell Lines. Human WNK4 cDNA was isolated by RT-PCR using human kidney mRNA as a template. The cDNA was cloned into the pTRE2-hyg vector (Clontech) and a C-terminal hemagglutinin (HA) tag was added. We also generated a WNK4 construct with an N-terminal Flag-tag. The disease-causing mutation (D564A) was introduced with the QuikChange site-directed mutagenesis kit (Stratagene). Stable cell lines were isolated by using Tet-off MDCK II cells (Clontech) as a host cell line with selection by using hygromycin B (200 μg/ml). Cell lines were screened by immunoblotting. Rat anti-HA mAb (9Y10) (Roche Diagnostics) and mouse M2 mAb or rabbit anti-Flag Ab (Sigma) were used to detect HA-tagged and Flag-tagged proteins, respectively. Endogenous claudins and occludin were detected with specific Abs (Zymed).

Measurement of Paracellular Na and Cl Permeability. Cells were seeded into a Millicell-HA filter (12-mm diameter; Millipore). When the cells were confluent, expression of transgenes was induced for 4 days by the removal of doxycycline. Tracer-flux experiments were performed in a solution containing 150 mM NaCl, 5 mM KCl, 2 mM $CaCl_2$, 1.5 mM $MgCl_2$, and 10 mM

This paper was submitted directly (Track II) to the PNAS office.

Abbreviations: PHAII, pseudohypoaldosteronism type II; TSC, Na-dependent Cl cotransporter; MDCK II, Madin–Darby canine kidney II; HA, hemagglutinin.

*To whom correspondence should be addressed. E-mail: suchida.kid@tmd.ac.jp.

www.pnas.org/cgi/doi/10.1073/pnas.0306924101

Hepes·NaOH (pH 7.4). We added 1 μCi/ml (1 Ci = 37 GBq) ^{22}Na or 5 μCi/ml ^{36}Cl to the medium on one side of the membrane, and the appearance of radioactivity in the medium on the other side was measured at various times. The composition of medium on both sides of the membrane was identical. When ^{36}Cl was used, cold NaCl was added to the medium on the other side of the membrane because the concentration of NaCl in ^{36}Cl tracer was high (≈1.6 M). We measured ^{22}Na and ^{36}Cl activity with a gamma counter and a liquid scintillation counter, respectively. Permeabilities for ^{22}Na and ^{36}Cl were calculated by using the following equation: $J_{Cl} = C_{Cl} \times P_{Cl} \times A$, where J_{Cl} is transepithelial Cl flux (mol/s), C_{Cl} is concentration (mol/liter), A is surface area (cm^2), and P is permeability. Statistical comparison of multiple groups was assessed by ANOVA. Chloride permeabilities in the WNK4 expressing cells between uninduced and induced states were compared by using a paired t test. Error bars are represent mean ± SEM. Statistical significance was defined at $p < 0.05$.

Phosphorylation of Claudins. Mammalian expression vectors (3× Flag CMV14; Sigma) encoding Flag-tagged claudins and occludin were generated by RT-PCR. Both wild-type and mutant WNK4 expression vectors and claudin expression vectors were cotransfected into COS7 and MDCK II cells with Lipofectamine 2000 (Invitrogen). At 24 h after transfection, cells were incubated for 2 h in phosphate-free DMEM with 0.5% BSA and 10 mM Hepes (pH 7.4). The cells were incubated further for 2 h in the same medium containing [^{32}P]P_i (1 mCi/ml). After incubation, the cells were washed with phosphate-free DMEM, harvested, and lysed for 1 h on ice in 150 mM NaCl/15 mM Tris·HCl,/25 mM NaF/1 mM Na_3VO_4 (pH 8.0). Proteins were immunoprecipitated with anti-Flag M2 Ab. Western blot analyses of the immunoprecipitates were performed also by using an anti-Flag polyclonal Ab to confirm the expression of claudins. To detect the phosphorylation of endogenous claudins, immunoprecipitation of claudins in the WNK4-expressing MDCK II cells was performed by using anti-claudin 1 and 4 Abs (Zymed). Immunoprecipitated proteins were separated by SDS/PAGE, and phosphorylated proteins were visualized by autoradiography.

For *in vitro* kinase assays, a GST-fusion protein containing the kinase domain of WNK4 was generated by subcloning the *SalI–MstI* fragment of WNK4 into pGEX6P-1 (Amersham Biosciences). The cytoplasmic region of claudin 4 was also generated as a GST-fusion protein for uses as a substrate of WNK4. Protein kinase reactions were carried out at 30°C for 15 min in kinase buffer (10 mM Tris, pH 7.4/150 mM NaCl/10 mM $MgCl_2$/0.5 mM DTT). Reaction mixtures were resolved by SDS/PAGE, and phosphorylated proteins were visualized by autoradiography.

Coimmunoprecipitation of WNK4 and Claudins. HA-tagged WNK4 and Flag-tagged claudins expressed in COS7 and MDCK II cells were immunoprecipitated with anti-Flag M2 Ab, and coprecipitation was examined by Western blotting with an anti-HA Ab. The interaction of HA-WNK4 and endogenous tight-junction proteins in the WNK4-expressing MDCK II cells was examined by immunoprecipitation by using an anti-HA Ab, followed by Western blotting using Abs to tight-junction proteins (Zymed).

Results

WNK4 Increases Paracellular Cl Permeability in MDCK Cells. We generated stable MDCK II cell lines expressing the wild-type and one of the human disease-causing mutants (D564A) of WNK4 by using a tetracycline-inducible system. We measured the transepithelial paracellular ^{22}Na and ^{36}Cl permeability of these cells grown on a permeable support. Before measuring the Na and Cl permeability, expression of the wild-type and the mutant WNK4

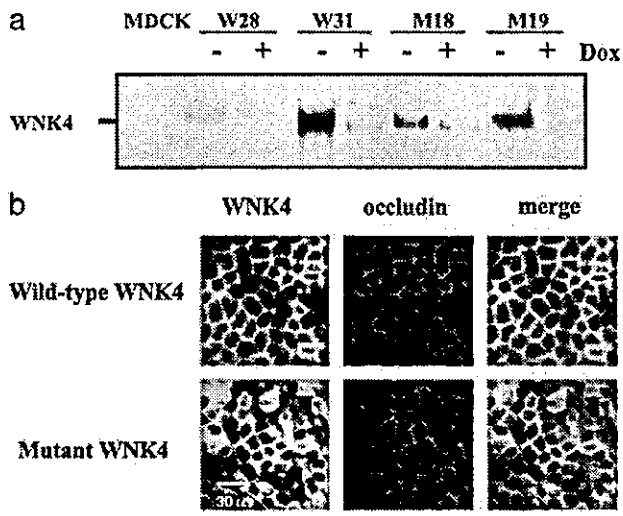

Fig. 1. Generation of wild-type and mutant WNK4-expressing MDCK II cell lines. (*a*) Expression of wild-type and mutant WNK4 in MDCK II cells. HA-tagged WNK4 proteins were detected by using an anti-HA (9Y10) Ab. Expression of WNK4 was induced by removal of doxycycline from the medium for 4 days. W28 and W31 are wild-type WNK4-expressing cell lines, and M18 and M19 are mutant WNK4-expressing cell lines. (*b*) Immunofluorescence of wild-type and mutant WNK4 expressed in isolated stable cell lines. Cells were grown on a permeable support, and the expression of WNK4 was induced for 4 days. WNK4 was detected by using an anti-HA Ab in conjunction with an Alexa 546-conjugated anti-rat IgG Ab. Cells were stained for occludin by using an anti-occludin Ab (Zymed) in conjunction with an Alexa 488-conjugated anti-rabbit IgG Ab.

were confirmed by Western blot analysis and immunofluorescence microscopy. As shown in Fig. 1*a*, stable cell lines expressing the wild-type and the mutant WNK4 were isolated. In all cell lines, some expression, even in the presence of doxycycline, was observed. Accordingly, we performed the initial experiments in induced cells (doxycycline-negative). Intracellular localization of the wild-type and the mutant WNK4 colocalized with the tight-junction protein occludin but did not appear to be different between the two cell lines (Fig. 1*b*). This localization of WNK4 in tight junctions is consistent with the reported (1) association of wild-type WNK4 with tight junctions *in vivo*. Flag-tagged WNK4 and HA-tagged WNK4 did not show the difference in terms of their cellular localization (data not shown).

We isolated several transformants after transfection with the empty vector, as well as the wild-type and mutant WNK4 cDNAs. We chose the four cell lines with the highest expression of the transgenes. Each cell line was cultured on a permeable support and was grown to confluence. Expression of WNK4 was induced for 4 days by removal of doxycycline from the medium. Transepithelial Na and Cl permeability were determined by assessing transepithelial ^{22}Na and ^{36}Cl flux across the epithelium. In these assays, the medium composition on both sides of the membrane was identical. Radioisotope was added to the basal side of the membrane, and the appearance of radioisotope in the apical medium was measured over time. Our preliminary experiments revealed that Na and Cl flux was linear for 45 min. Therefore, we adopted 30 min as an incubation time for subsequent experiments. The calculated basal to apical permeability was identical to the apical to basal permeability. Addition of 1 mM ouabain/0.1 mM bumetanide/0.1 mM amiloride/0.1 mM hydrochlorothiazide/1 mM 4,4′-diisothiocyanatostilbene-2,2′-disulfonic acid/1 mM 4-acetamido-4′-isothiocyanatostilbene-2,2′-disulfonic acid had no effect on Na or Cl flux. In addition, Na and Cl fluxes measured in this assay appeared not to saturate

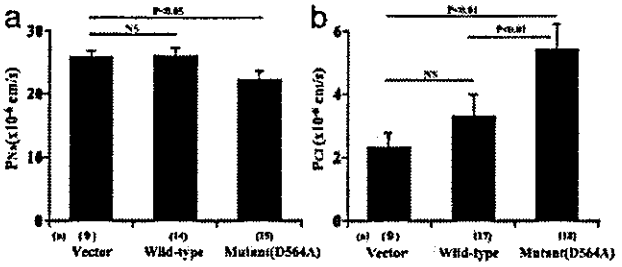

Fig. 2. Transepithelial ^{22}Na (*a*) and ^{36}Cl (*b*) permeability in MDCKII cells expressing wild-type and mutant WNK4. Each bar represents experiments using at least three cell lines. The numbers of assays are given in parentheses. At least three assays were performed with each cell line.

as a function of NaCl concentration up to 200 mM. These results (see Figs. 6 and 7, which are published as supporting information on the PNAS web site) suggest that our measurements represent paracellular Na and Cl permeability of the epithelium. Our permeability calculations [P (Na) = 25.8 ± 0.9 cm/s (mean ± SEM, n = 7), P (Cl) = 2.0 ± 0.3 cm/s (mean ± SEM, n = 11) in the host cells] also agreed with calculations made previously by using other methods (10). These calculated permeabilities suggest that our simplified assay is valid for measuring transepithelial Na and Cl permeability.

As shown in Fig. 2*a*, Na permeability was not changed by the expression of the wild-type WNK4 compared with the vector transfection. However, the mutant WNK4 causes a statistically significant decrease in Na permeability ($p < 0.05$). The Cl permeability in the wild-type WNK4-expressing cell lines tended to be increased over the control (empty-vector transfectants), but the difference was not statistically significant. In the two wild-type WNK4-transfected cell lines that showed the least leaky WNK4 expression in the presence of doxycycline, chloride permeabilities under induced and noninduced conditions were not statistically different. On the other hand, the mutant WNK4 caused an apparent increase in Cl permeability ($p < 0.01$) over the control and also over the wild type ($p < 0.01$). This increase of chloride permeability was not due to a general increase of permeability of the epithelia because Na permeability was reduced. To further confirm that the increase in chloride permeability in the mutant WNK4-expressing cells correlated with the expression of the mutant WNK4, we chose the two mutant WNK4-transfected cell lines that showed the least leaky WNK4 expression. In those cells, chloride permeability under the induced and noninduced conditions was 5.8 ± 0.4 and 2.8 ± 0.2 ($\times 10^{-6}$ cm/s), respectively, which were statistically significant (mean ± SEM, n = 6, $p < 0.01$).

Effect of WNK4 Expression on Cellular Localization of Tight-Junction Proteins. We suspected that WNK4 expression enhanced Cl permeability by modifying proteins in the tight junction. We first performed immunofluoresence and Western blot analyses of tight-junction proteins to determine whether there was any difference in expression or localization. Fig. 3*a* shows the immunofluorescence staining for several claudins and occludin. The localization of these proteins in the tight junctions did not appear to be affected by wild-type or mutant WNK4 expression. Because the recruitment of some proteins to the tight junctions, including occludin, claudins, and ZO-1, are regulated by various signals (11), we examined their distribution in the Triton X-100-soluble (cytosol) and -insoluble (cytoskeleton and tight junctions) cellular fractions by Western blotting. As shown in Fig. 3*b*, the distribution of the claudins into Triton X-100-insoluble fraction was not significantly altered by the expression of wild-type or mutant WNK4, although two of four wild-type WNK4–

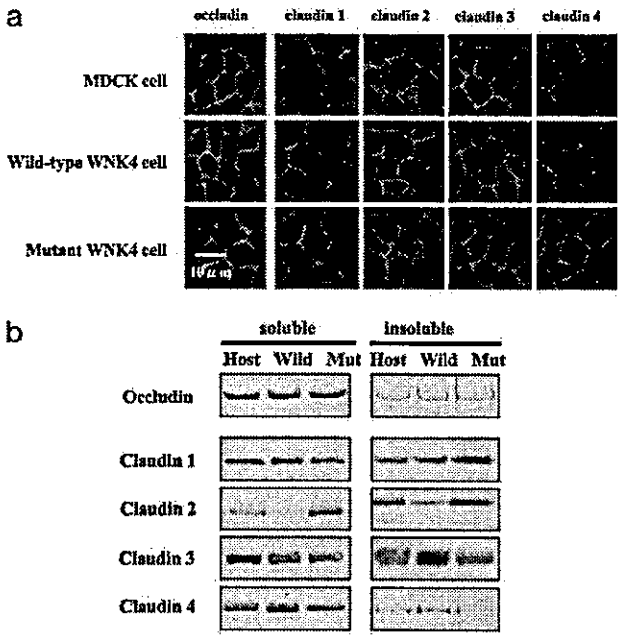

Fig. 3. Tight-junction proteins in WNK4-expressing cells. (*a*) Immunofluorescence of tight-junction proteins in the WNK4-expresing cells. Stable WNK4-expressing cell lines were grown on a permeable support. Cells were immunostained with anti-claudin 1–4 Abs or with an anti-occludin Ab. (*b*) Expression of claudins and occludin in Triton X-100-soluble and -insoluble fractions in WNK4-expressing cells. WNK4 expression was induced for 4 days, and cells were harvested in a buffer containing 1% Triton X-100. The Triton X-100-soluble and -insoluble fractions were resolved by SDS/PAGE, and the expression of claudins and occludin were determined by Western blot analysis.

expressing cell lines displayed decreased claudin 2 expression. A similar reduction in claudin 2 expression was reported (12) in cells overexpressing claudin 8, although that was thought to be an artifact of overexpression. We, therefore, concluded that the increased Cl permeability in WNK4-expressing cells was not caused by changes in the recruitment of tight-junction proteins.

Increased Phosphorylation of Claudins Induced by WNK4 Overexpression. We next investigated whether the change in Cl permeability was associated with modification of the tight-junction proteins (i.e., phosphorylation). Because commercially available Abs for claudins are not always effective for immunoprecipitation, we initially examined the phosphorylation of Flag-tagged claudins. We first used COS7 cells to obtain consistent expression of exogenous claudins. Fig. 4*a* shows that all claudins tested (claudin 1–4) were phosphorylated in cells expressing WNK4. Cells expressing mutant WNK4 contained a higher level of phosphorylated claudin than cells expressing wild-type WNK4. Occludin, an endogenously phosphorylated tight-junction protein, was not phosphorylated further in cells expressing either the wild-type or the mutant WNK4. Less phosphorylation of claudins by the wild-type WNK4 than the mutant, and the lack of further phosphorylation of occludin by WNK4 suggested that the phosphorylation of claudins by the mutant WNK4 was not due to an artifact of overexpression. The same results were obtained in MDCK II cells (Fig. 4*b*). To further confirm these results, we also checked the phosphorylation of endogenous claudins in the WNK4-expressing MDCK cells. As shown in Fig. 4*c*, endogenous claudin 1 and claudin 4 were apparently phosphorylated in the mutant-expressing MDCK II cells, identifying a putative molecular target for this protein kinase. We also examined the level of WNK4 phosphorylation because WNK1 is known to autophos-

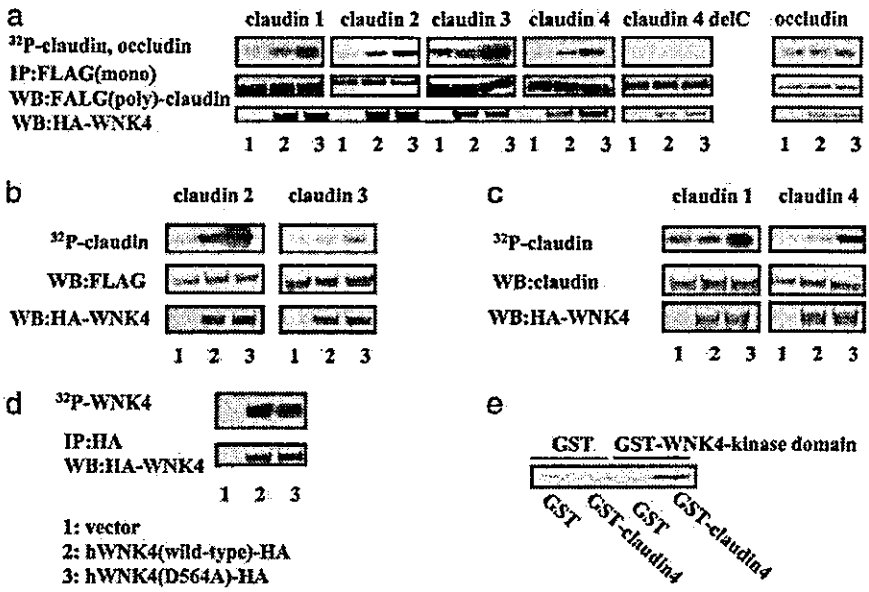

Fig. 4. Phosphorylation of claudins by WNK4. (*a*) Phosphorylation of Flag-tagged claudins by WNK4 in COS7 cells. COS7 cells were transfected with HA-tagged WNK4 and Flag-tagged claudins or occuludin. Claudin 4 delC lacks the entire C-terminal cytosolic region of claudin4. Cells were labeled with [^{32}P]P_i (1 mCi/ml), and proteins were immunoprecipitated with an anti-Flag Ab (M2). The immunoprecipitated Flag-claudins were separated by SDS/PAGE, electrophoretically transferred to nitrocellulose, and analyzed by Western blotting with an anti-Flag polyclonal Ab. After detecting the immunoprecipitated claudins, claudin phosphorylation was detected by autoradiography of the nitrocellulose membrane. (*b*) Phosphorylation of Flag-tagged claudins in the WNK4-expressing MDCK II cells. MDCK II cells stably expressing HA-tagged WNK4 were transfected with Flag-tagged claudin 2 and 3. Phosphorylated claudin 2 and 3 were detected, as described in *a*. (*c*) Phosphorylation of endogenous claudins in the mutant WNK4-expressing MDCK II cells. The WNK4-expressing cells were labeled with [^{32}P]P_i, and the endogenous claudins were immunoprecipitated by using anti-claudin 1 and 4 Abs (Zymed). Phosphorylation of claudins was visualized by autoradiography. (*d*) Phosphorylation of wild-type and mutant WNK4. MDCK II cells were transfected with HA-tagged wild-type and mutant WNK4. Cells were labeled with [^{32}P]P_i, and WNK4 proteins were immunoprecipitated with an anti-HA Ab. Immunoprecipitated proteins were resolved on SDS/PAGE, electrophoretically transferred to nitrocellulose, and analyzed by Western blotting with an anti-HA Ab. WNK4 phosphorylation was detected by autoradiography. (*e*) *In vitro* kinase assay with GST-WNK4. GST-WNK4 (kinase domain) and GST–claudin 4 (C-terminal cytoplasmic domain) were incubated at 37°C for 15 min in kinase buffer, and the phosphorylation of GST–claudin 4 was visualized by SDS/PAGE, followed by autoradiography.

phorylate (13, 14). As shown in Fig. 4*d*, there was an equal level of phosphorylation on wild-type and mutant WNK4. Finally, to verify that claudins were direct substrates for WNK4, we performed an *in vitro* kinase assay by using recombinant GST-fusion proteins of the kinase domain of WNK4 and the cytoplasmic domain of claudin 4. As shown in Fig. 4*e*, WNK4 directly phosphorylated the cytoplasmic domain of claudin 4.

Protein–Protein Interaction of WNK4 and Claudins. Our results clearly show that WNK4, especially the mutant WNK4, can phosphorylate claudins. Moreover, it appears that the mutant WNK4 has an enhanced ability to phosphorylate these proteins. To investigate this possibility further, we first examined whether WNK4 associates with the claudins. As expected from the phosphorylation study, claudins and WNK4 coimmunoprecipitated (Fig. 5*a*). The mutant WNK4 showed a much higher association with claudins than the wild-type WNK4. Because our analyses of WNK4 phosphorylation suggested that the wild-type and mutant proteins possess the same level of autophosphorylation (Fig. 4*d*) and, therefore, the same kinase activities, it appears that the enhanced phosphorylation of claudins by mutant WNK4 is due to the increased claudin–WNK4 association. Interaction of the mutant WNK4 with the endogenous claudin 1 and 4 but not with ZO-1 and occludin was confirmed in the mutant-expressing MDCK II cells (Fig. 5*b*).

In our phosphorylation studies (Fig. 4*a*), we found that deletion of the entire cytoplasmic C terminus of claudin 4 eliminated its phosphorylation, suggesting that the C terminus is the site of phosphorylation and/or binding by WNK4. Fig. 5*c* confirms that this C-terminal deletion mutant lost its ability to bind to the mutant WNK4, but that the addition of the C-terminal YV, a sequence highly conserved in all claudins (a binding site to PDZ domains of ZO-1, 2, and 3) (15), restored binding to the mutant WNK4. This finding indicates that the YV sequence is necessary for claudin binding and explains the fact that the mutant WNK4 binds all of the claudins tested. Phosphorylation of this mutant was not restored by the addition of YV motif (data not shown), suggesting that phosphorylation sites were present within the cytosolic C terminus.

Discussion

Two findings are presented in this article. First, we identified claudins as molecular targets of the protein kinase WNK4, especially the disease-causing mutant WNK4. Second, we show that paracellular ion permeability is regulated by the mutant WNK4. This study characterizes WNK4 expressed in polarized epithelial cells, and both data are quite consistent with the *in vivo* localization of WNK4 and the chloride shunt hypothesis in PHAII.

A growing body of evidence, including genetic (16) and cell biological (10, 12, 17–20) data, has suggested that paracellular transepithelial transport is important in vectorial ion and solute transport across the epithelia. Thus, it appears that, like channels, paracellular transport possesses selectivity for ions and solutes. Although several lines of evidence have suggested that claudins are the major determinants of paracellular ion selectivity (10, 12, 17–20), their phosphorylation has not, to our knowledge, been demonstrated. Our data showed a good correlation between increased chloride permeability and claudin phosphorylation induced by the mutant WNK4, suggesting that

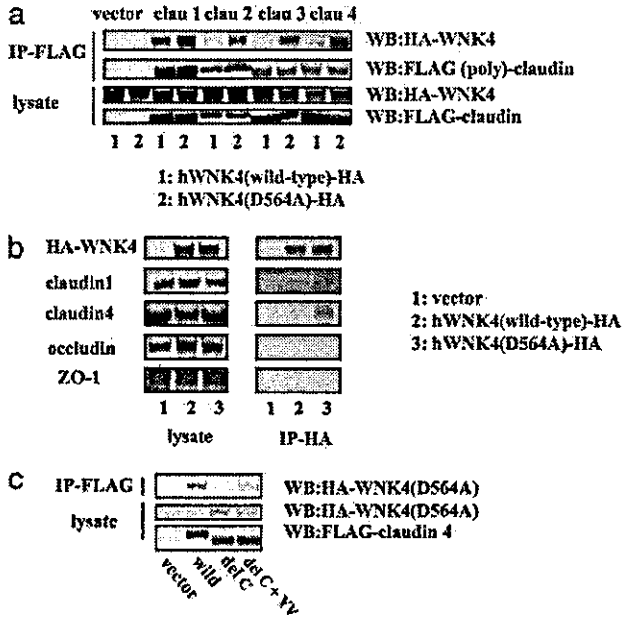

Fig. 5. Analysis of WNK4–claudin interaction. (*a*) Coimmunoprecipitation of WNK4 and claudins. COS7 cells were transfected with HA-tagged WNK4 and Flag-tagged claudins. Proteins were immunoprecipitated with an anti-Flag M2 Ab, and the immunoprecipitates were analyzed by Western blot analysis by using anti-HA Ab. (*b*) Coimmunoprecipitation of WNK4 and endogenous tight-junction proteins. Proteins from MDCK II cells stably expressing the wild-type and mutant HA-WNK4 were immunoprecipitated with anti-HA Ab, and the immunoprecipitates were analyzed by Western blot analysis by using Abs to claudin 1, claudin 4, ZO-1, and occludin. (*c*) Binding of claudin 4 and its mutants by mutant WNK4. Claudin 4 binding was assessed by coimmunoprecipitation in lysates from MDCK II cells as described in *a*. Mutants examined include delC (the claudin 4 mutant lacking the entire C terminal cytoplasmic region) and del C plus YV (the del C mutant with Y and V added to the C terminus). Addition of YV residues restored the binding to WNK4.

the two phenomena are related causally. However, whether the phosphorylation of claudins causes an increase in the chloride permeability directly remains to be determined. A mutagenesis study showed that the extracellular domain of claudin controls paracellular charge selectivity and resistance (10). However, it is not clear now whether the phosphorylation of the cytoplasmic domain affects chloride permeability. Currently, there is no good system, to our knowledge, for assaying the function of exogenously expressed claudins in mammalian cells because of the presence of numerous endogenous claudins. We can only speculate that the phosphorylation by WNK4 affects the conformation of claudins, increasing Cl ion pore permeability or affecting their interaction with intracellular regulators, such as cytoskeletal proteins.

We found in this study that the disease-causing mutation in WNK4 has a gain-of-function effect, causing increased chloride permeability and hyperphosphorylation of claudins. This finding provides a good explanation for the autosomal-dominant nature of inheritance in PHAII. Very recently, Kahle *et al.* (6) reported the inhibition of surface expression of the renal K^+ channel ROMK by coexpression of wild-type WNK4 in *Xenopus* oocytes. Interestingly, a disease-causing mutation in WNK4 that relieves TSC inhibition (4, 5) markedly increases inhibition of ROMK. This difference in the action of the mutant WNK4 on TSC and ROMK indicates that WNK4 functions as a multifunctional regulator of diverse ion transporters. Identification of functions of WNK4 in this study further supports this notion. However, how this mutation increases WNK4 activity is not clear, as in the case of ROMK inhibition. In terms of claudin phosphorylation, one possible explanation for the enhanced effect of the mutant is change in the binding to claudins. In fact, Xu *et al.* (14) recently reported the presence of an autoinhibitory domain in WNK1 that resides near the coil domain. Interestingly, PHAII-causing mutations are concentrated near the putative autoinhibitory domain of WNK4. Therefore, it is possible that the disease-causing mutations in WNK4 somehow affect its interaction with its negative regulators including its own domains, releasing the active site, and allowing enhanced binding to claudins. Although we show that YV motif of claudins is important for the interaction with WNK4, further work will be required to define the whole mechanisms of their interaction.

In this article, we identified the claudins as targets of WNK4 kinase and showed that the disease-causing mutant WNK4 expression increases paracellular chloride permeability without increasing sodium permeability. A similar phenomenon may occur in the collecting ducts of PHAII patients. Therefore, increased chloride shunt caused by a gain-of-function activity of mutant WNK4 may underlie or contribute to the pathogenesis of PAHII.

We thank H. Ichijo (Tokyo University) for his excellent advice. This study was supported in part by grants-in-aid from the Ministry of Education, Culture, Sports, Science, and Technology of Japan and the Salt Science Research Foundation.

1. Wilson, F. H., Disse-Nicodeme, S., Choate, K. A., Ishikawa, K., Nelson-Williams, C., Desitter, I., Gunel, M., Milford, D. V., Lipkin, G. W., Achard, J. M., *et al.* (2001) *Science* **293**, 1107–1112.
2. Schambelan, M., Sebastian, A. & Rector, F. C., Jr. (1981) *Kidney Int.* **19**, 716–727.
3. Farfel, Z., Iaina, A., Rosenthal, T., Waks, U., Shibolet, S. & Gafni, J. (1978) *Arch. Intern. Med. (Moscow)* **138**, 1828–1832.
4. Wilson, F. H., Kahle, K. T., Sabath, E., Lalioti, M. D., Rapson, A. K., Hoover, R. S., Hebert, S. C., Gamba, G. & Lifton, R. P. (2003) *Proc. Natl. Acad. Sci. USA* **100**, 680–684.
5. Yang, C. L., Angell, J., Mitchell, R. & Ellison, D. H. (2003) *J. Clin. Invest.* **111**, 1039–1045.
6. Kahle, K. T., Wilson, F. H., Leng, Q., Lalioti, M. D., O'Connell, A. D., Dong, K., Rapson, A. K., MacGregor, G. G., Giebisch, G., Hebert, S. C. & Lifton R. P. (2003) *Nat. Genet.* **35**, 372–376.
7. Schuster, V. L. & Stokes, J. B. (1987) *Am. J. Physiol.* **253**, F203–F212.
8. Plotkin, M. D., Kaplan, M. R., Verlander, J. W., Lee, W. S., Brown, D., Poch, E., Gullans, S. R. & Hebert, S. C. (1996) *Kidney Int.* **50**, 174–183.
9. Xu, J. Z., Hall, A. E., Peterson, L. N., Bienkowski, M. J., Eessalu, T. E. & Hebert, S. C. (1997) *Am. J. Physiol.* **273**, F739–F748.
10. Colegio, O. R., Itallie, C. V., Rahner, C. & Anderson, J. M. (2003) *Am. J. Physiol.* **284**, C1346–C1354.
11. Nishiyama, R., Sakaguchi, T., Kinugasa, T., Gu, X., MacDermott, R. P., Podolsky, D. K. & Reinecker, H. C. (2001) *J. Biol. Chem.* **276**, 35571–35580.
12. Yu, A. S., Enck, A. H., Lencer, W. I. & Schneeberger, E. E. (2003) *J. Biol. Chem.* **278**, 17350–17359.
13. Xu, B., English, J. M., Wilsbacher, J. L., Stippec, S., Goldsmith, E. J. & Cobb, M. H. (2000) *J. Biol. Chem.* **275**, 16795–16801.
14. Xu, B. E., Min, X., Stippec, S., Lee, B. H., Goldsmith, E. J. & Cobb, M. H. (2002) *J. Biol. Chem.* **277**, 48456–48462.
15. Itoh, M., Furuse, M., Morita, K., Kubota, K., Saitou, M. & Tsukita, S. (1999) *J. Cell Biol.* **147**, 1351–1363.
16. Simon, D. B., Lu, Y., Choate, K. A., Velazquez, H., Al-Sabban, E., Praga, M., Casari, G., Bettinelli, A., Colussi, G., Rodriguez-Soriano, J., *et al.* (1999) *Science* **285**, 103–106.
17. Amasheh, S., Meiri, N., Gitter, A. H., Schoneberg, T., Mankertz, J., Schulzke, J. D. & Fromm, M. (2002) *J. Cell Sci.* **115**, 4969–4976.
18. Colegio, O. R., Van Itallie, C. M., McCrea, H. J., Rahner, C. & Anderson, J. M. (2002) *Am. J. Physiol.* **283**, C142–C147.
19. Furuse, M., Furuse, K., Sasaki, H. & Tsukita, S. (2001) *J. Cell Biol.* **153**, 263–272.
20. Van Itallie, C., Rahner, C. & Anderson, J. M. (2001) *J. Clin. Invest.* **107**, 1319–1327.

Research article

Inhibition of diabetic nephropathy by a decoy peptide corresponding to the "handle" region for nonproteolytic activation of prorenin

Atsuhiro Ichihara,[1] Matsuhiko Hayashi,[1] Yuki Kaneshiro,[1] Fumiaki Suzuki,[2,3] Tsutomu Nakagawa,[2] Yuko Tada,[1] Yukako Koura,[1] Akira Nishiyama,[4] Hirokazu Okada,[5] M. Nasir Uddin,[2] A.H.M. Nurun Nabi,[3] Yuichi Ishida,[6] Tadashi Inagami,[7] and Takao Saruta[1]

[1]Department of Internal Medicine, Keio University School of Medicine, Tokyo, Japan. [2]Faculty of Applied Biological Sciences, [3]United Graduate School of Agricultural Science, Gifu University, Gifu, Japan. [4]Department of Pharmacology, Kagawa Medical School, Kagawa, Japan. [5]Nephrology, Saitama Medical College, Saitama, Japan. [6]Prevaqol Co., Tokyo, Japan. [7]Department of Biochemistry, Vanderbilt University School of Medicine, Nashville, Tennessee, USA.

We found that when a site-specific binding protein interacts with the "handle" region of the prorenin prosegment, the prorenin molecule undergoes a conformational change to its enzymatically active state. This nonproteolytic activation is completely blocked by a decoy peptide with the handle region structure, which competitively binds to such a binding protein. Given increased plasma prorenin in diabetes, we examined the hypothesis that the nonproteolytic activation of prorenin plays a significant role in diabetic organ damage. Streptozotocin-induced diabetic rats were treated with subcutaneous administration of handle region peptide. Metabolic and renal histological changes and the renin-Ang system components in the plasma and kidneys were determined at 8, 16, and 24 weeks following streptozotocin treatment. Kidneys of diabetic rats contained increased Ang I and II without any changes in renin, Ang-converting enzyme, or angiotensinogen synthesis. Treatment with the handle region peptide decreased the renal content of Ang I and II, however, and completely inhibited the development of diabetic nephropathy without affecting hyperglycemia. We propose that the nonproteolytic activation of prorenin may be a significant mechanism of diabetic nephropathy. The mechanism and substances causing nonproteolytic activation of prorenin may serve as important therapeutic targets for the prevention of diabetic organ damage.

Introduction

The most striking abnormalities of the renin-Ang system (RAS) in the blood of diabetic animals are the decreased renin level and the increased prorenin level (1). Indeed, increased blood prorenin levels in human diabetics have been reported to predict microvascular complications (2). Recent studies have demonstrated that transgenic rats expressing prorenin have severe renal histopathology mimicking diabetic nephrosclerosis without hypertension (3) and show evidence that circulating prorenin may enter organs (4). The mechanism whereby intracellular prorenin causes organ damage remained unclear, however.

Prorenin has a prosegment of 43 amino acid residues attached to the N terminus of mature (active) renin, and the prosegment folds into an active site cleft of mature renin to prevent catalytically productive interaction with angiotensinogen. When a prorenin-binding protein interacts with the "handle" region of the prorenin prosegment, the prorenin molecule undergoes a conformational change to an enzymatically active state (5). This phenomenon is called nonproteolytic activation, and such binding proteins include a specific Ab to the prosegment (5), the *N*-acyl-D-glucosamine 2-epimerase (6), the mannose-6-phosphate receptor (7, 8), or the prorenin/renin receptor (9). These findings indicate the strong possibility that a peptide with the structure of this handle region (handle region peptide, or HRP; see Figure 1) must competitively bind to such a binding protein as a decoy peptide and inhibit the nonproteolytic activation of prorenin.

In the present study, we used such a decoy peptide to demonstrate a novel mechanism whereby prorenin as such, without proteolytic activation, causes organ damage by comparing levels of the RAS components in the kidney and plasma during the development of diabetic nephropathy. HRP clearly prevented development of diabetic nephropathy and suppressed an increase of renal Angs while the total renal renin plus prorenin remained unaltered. To clarify the mechanism whereby prorenin causes organ damage, we investigated the alteration of the RAS component levels in the plasma and kidneys during the development of diabetic nephropathy and the in vitro and in vivo effects of HRP on their alteration levels.

Results

In vitro effects of HRP on binding of prorenin to prorenin Abs. To examine the affinity, specificity, and dose of HRP in the inhibitory effects on the binding of rat prorenin to its Abs, immunoblot analysis of recombinant prorenin to the Ab for the anti-handle region was performed. The binding of recombinant prorenin to the Ab for the anti-handle region was completely inhibited by 1 μM HRP (RILLKKMPSV) but was not influenced by the peptides representing other regions of the prorenin prosegment (SFGR or MTRISAE) (Figure 2A). Similar results were also obtained at 10 and 100 nM HRP. In

Nonstandard abbreviations used: ACE, Ang-converting enzyme; C rat, nondiabetic control rat with saline minipump; C + HRP rat, nondiabetic control rat with HRP-containing minipump; DM + HRP rat, diabetic rat with HRP minipump; DM rat, diabetic rat with saline-containing minipump; HRP, handle region peptide; RAS, renin-Ang system.

Conflict of interest: The authors have declared that no conflict of interest exists.

Citation for this article: *J. Clin. Invest.* 114:1128–1135 (2004). doi:10.1172/JCI200421398.

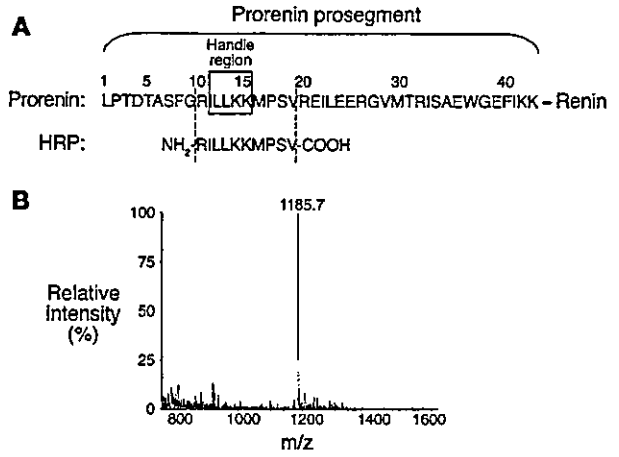

Figure 1
Preparation of the decoy peptide corresponding to the HRP. (**A**) Amino acid sequences of the rat prorenin prosegment and HRP. (**B**) Mass of the HRP prepared.

addition, HRP did not affect the binding of prorenin to Ab against proteolytically activated renin (Figure 2B). These results suggest that HRP can specifically bind to the anti-HRP Ab with a high affinity and inhibit the binding of prorenin to anti-HRP Ab in vitro.

During in vitro preliminary experiments, we had expressed rat prorenin/renin receptor protein (accession number AB188298 in the DNA Databank of Japan) in COS-7 cells and showed binding and activation of recombinant rat prorenin by 20% ± 2.5% of the trypsin-activatable level (350 ng Ang I/ml/hr). This activation was practically abolished by rat HRP (10P-19P) used as a decoy at 1 μM, but not by another prosegment heptapeptide (30P-36P) outside the handle region, indicating specific inhibitory action of HRP against prorenin activation. We also found that prorenin activated by rat prorenin/renin receptor expressed on COS-7 cells could be bound to anti-rat HRP Abs on the cells, visualized by using intensifying second Ab conjugated with peroxidase. This result indicated that prorenin activated by the receptor protein still had a prosegment including the handle region and that activation of prorenin by the receptor protein was presumably not due to a proteolytic mechanism but was due to a conformational change. Analogous to the prorenin/renin-binding protein, polyclonal Abs to the rat HRP also activated rat prorenin by 20% ± 1.0% of the maximum activation attainable by trypsin, and the activation was practically abolished by 1 μM HRP used as a decoy. These results indicate that specific binding of prorenin either to the receptor protein or Ab to HRP results in a significant activation of prorenin. These observations provide in vitro evidence that HRP inhibits the activation by competing out the binding of the prorenin receptor or HRP Abs to prorenin.

Metabolic changes and urinary protein excretion. We determined metabolic changes and urinary protein excretion in nondiabetic control rats with saline minipumps (C rats), nondiabetic control rats with HRP-containing minipumps (C + HRP rats), diabetic rats with saline-containing minipumps (DM rats), and diabetic rats with HRP minipumps (DM + HRP rats) during the 24-week treatment period (Figure 3). The body weight of the DM rats averaged 231 ± 15 g at 28 weeks of age and was significantly smaller than that of the C rats (590 ± 10 g). The basal BP of the C and DM rats averaged 123 ± 2 and 122 ± 2 mmHg, respectively, and the BP had been similar in the C and DM rats during the 24-week treatment period. The blood glucose levels of the DM rats averaged 509 ± 34 mg/dl at 8 weeks of age (4 weeks of diabetes) and was significantly higher than those of the C rats (132 ± 14 mg/dl). Higher blood glucose levels of the DM rats versus the C rats were maintained during the 24-week treatment period. Continuous infusion of HRP by subcutaneous minipumps did not affect the body weight, BP, or blood glucose levels of either control or diabetic rats during the 24-week treatment period, although the body weight of diabetic rats increased at 24 and 28 weeks of age. In the DM rats, urinary protein excretion significantly increased from 20.0 ± 3.1 at 4 weeks of age (0 weeks of diabetes) to 118.8 ± 11.9 mg/day at 28 weeks of age (24 weeks of diabetes), and HRP practically normalized the increased urinary protein excretion in diabetic rats to levels similar to those of the control rats. The urinary protein excretion at 28 weeks of age (24 weeks of diabetes) in the DM + HRP rats averaged 33.0 ± 4.1 mg/day and was similar to that in the C and C + HRP rats.

Morphology and immunohistochemistry. Figure 4A shows changes in renal morphology in the C, C + HRP, DM, and DM + HRP rats during the 24-week treatment period. We did not observe any histological changes in the kidney of the DM rats up to 12 weeks of age (8 weeks of diabetes), but glomerulosclerosis began to develop at 20 weeks of age (16 weeks of diabetes) and was exacerbated at 28 weeks of age (24 weeks of diabetes). As shown in Figure 4B, the glomerulosclerosis index of 20- and 28-week-old DM rats averaged 1.25 ± 0.16 and 1.96 ± 0.14, respectively, and was significantly greater than that of the C, C + HRP, or DM + HRP rats. In the 28-week-old DM rats, the glomerulosclerosis index was significantly greater than that at 20 weeks of age. Long-term administration of HRP completely inhibited the development of glomerulosclerosis in the diabetic rats, and we did not observe any histological changes during the 24-week treatment period in the DM + HRP rats.

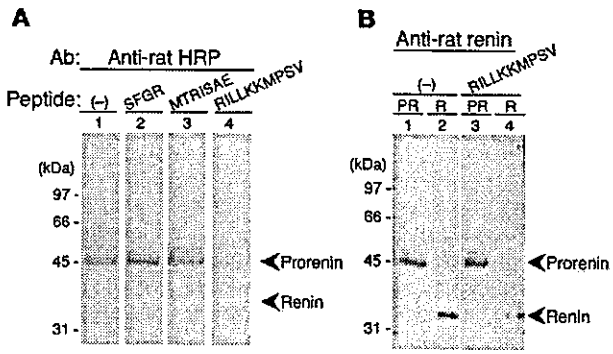

Figure 2
Interference of the prorenin binding to its Abs by the HRP. (**A**) Recombinant rat prorenin was analyzed by immunoblotting using 3 nM purified Ab to HRP in the absence (–; lane 1) or presence of 1 μM regional peptides of prorenin prosegment, SFGR (lane 2), MTRISAE (lane 3), or RILLKKMPSV (lane 4). The image shows that HRP binds to the anti–HRP Ab with a high affinity and inhibits the binding of recombinant prorenin to anti–HRP Ab. Similar results were also obtained at 10 and 100 nM RILLKKMPSV. (**B**) Recombinant rat prorenin (PR) (lanes 1 and 3) and renin (R) (lanes 2 and 4) were analyzed by immunoblotting using anti–rat renin Ab in the absence (lanes 1 and 2) or presence of 1 μM HRP, RILLKKMPSV (lanes 3 and 4). The image shows that HRP specifically binds to the anti–HRP Ab but not to the anti–renin Ab and does not inhibit the binding of prorenin to anti–renin Ab.

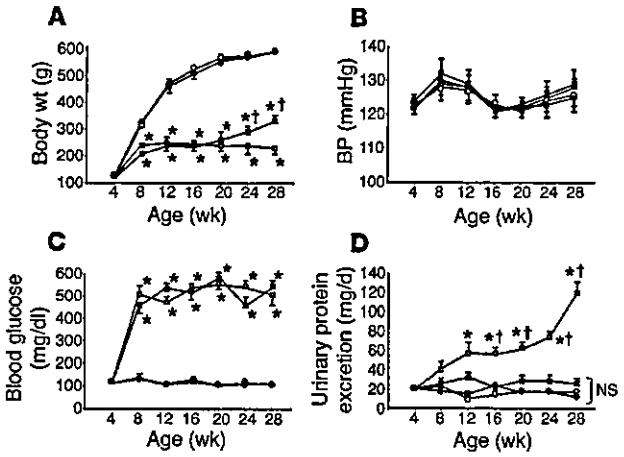

Figure 3

Metabolic changes and urinary protein excretion in C rats (open circles, $n = 18$), C + HRP rats (closed circles, $n = 18$), DM rats (open squares, $n = 18$), and DM + HRP rats (closed squares, $n = 18$). (**A**) Body weight. Graph shows attenuation of body weight gain in diabetic rats. Except for the increases at 24 and 28 weeks of age in diabetic rats, HRP did not affect body weight during the 24-week treatment period. *$P < 0.05$ versus C or C + HRP rats; †$P < 0.05$ for DM + HRP versus DM rats. (**B**) Systolic BP. The graph shows similar systolic BP in all 4 groups of rats. (**C**) Blood glucose concentration. The graph shows increased blood glucose levels in the diabetic rats. HRP had no effect on blood glucose levels. *$P < 0.05$ versus C or C + HRP rats. (**D**) Urinary protein excretion. The graph shows a progressive increase in urinary protein excretion in DM rats. HRP treatment inhibited the development and progression of proteinuria in diabetic rats. *$P < 0.05$ versus 4 weeks of age; †$P < 0.05$ for DM rats versus the other 3 groups. NS, no significant difference among the C, C + HRP, and DM + HRP rats.

The glomerulosclerosis index was similar among the C, C + HRP, and DM + HRP rats during the 24-week treatment period. We also investigated ECM accumulation in the kidney of diabetic rats by type IV collagen immunostaining, as shown in Figure 4C. Kidneys of all groups of rats were negative for expression of type IV collagen in the glomerulus up to 12 weeks of age, but at 20 weeks of age type IV collagen was expressed in the glomerulosclerotic lesions of the kidneys of the DM rats. At 28 weeks of age, expression of type IV collagen increased in the DM rats, but it was markedly suppressed to a level slightly higher than the control level in the DM + HRP rats ($n = 6$), though the difference between C rats and DM + HRP rats was statistically insignificant (Figure 4D). Expression of type IV collagen during the 24-week treatment period was not observed in either the C or C + HRP rats.

Components of the circulating and kidney RAS. As shown in Figure 5, plasma renin activity was significantly lower in the DM rats than in the C rats during the 24-week treatment period, and administration of HRP did not affect plasma renin activity in either control or diabetic rats (Figure 5A). Plasma prorenin level was significantly higher in the DM rats than in the C rats up to 20 week of age (16 weeks of diabetes), and administration of HRP did not affect plasma prorenin level in either control or diabetic rats (Figure 5B). The plasma levels of Ang I and II were also lower in the DM rats than in the C rats during the 24-week treatment period, and HRP did not influence plasma Ang I or II levels of either control or diabetic rats (Figure 5, C and D).

At 8 weeks of age (4 weeks of diabetes) when the diabetic nephropathy had not yet developed, the DM rats had a small but significant increase in the kidney Ang I and II content (109 ± 16 and 147 ± 12 fmol/g, respectively) compared with the C rats (58 ± 11 and 77 ± 8 fmol/g, respectively). At 12, 20, and 28 weeks of age, the kidney Ang I and II content was significantly higher in the DM rats than the similarly low levels in the C, C + HRP, and DM + HRP rats (Figure 6, A and B). The kidney Ang I content of the DM, DM + HRP, C, and C + HRP rats averaged 268 ± 51, 70 ± 8, 88 ± 14, and 71 ± 13 fmol/g, respectively, and the kidney Ang II content of the DM, DM + HRP, C, and C + HRP rats averaged 220 ± 21, 126 ± 15, 148 ± 14, and 124 ± 12 fmol/g, respectively, at 20 weeks of age (16 weeks of diabetes) when renal histological changes have developed. Thus, HRP administration completely inhibited the increased kidney Ang I and II content in the diabetic rats. The kidney total renin content and the kidney renin mRNA level were lower in the DM rats than in the C rats at 12 and 20 weeks of age, and they were similar at 28 weeks of age. HRP administration did not alter kidney total renin content or kidney renin mRNA levels in either control or diabetic rats at any week of age (Figures 6C and 7A). The kidney Ang-converting enzyme (ACE) and angiotensinogen mRNA levels were similar in the C, C + HRP, DM, and DM + HRP rats during the 24-week treatment period (Figure 7, B and C) but tended to decrease with age. The kidney cathepsin B mRNA level was significantly lower in the DM rats than in the C rats during the 24-week treatment period. HRP administration did not alter kidney cathepsin B mRNA level in either control or diabetic rats at any week of age (Figure 7D).

To estimate the kidney levels of prorenin and renin, we performed immunohistochemical analysis of the kidneys collected from rats diabetic for 24 weeks. The anti-rat HRP Ab and anti-rat renin Ab used in the present study bind to total prorenin and activated prorenin, respectively. Because the activated prorenin represents both proteolytically activated prorenin (i.e., renin) and nonproteolytically activated prorenin, the results of immunostaining can provide a hint regarding an activation of prorenin. The prorenin-positive cells were significantly greater in number in the juxtaglomerular area of DM rats compared with C rats. The increased prorenin immunoreactivity was not affected by the HRP treatment (Figure 8, A and B). The immunoreactivity of activated prorenin was also increased in the juxtaglomerular area of DM rats, but it was significantly decreased by the HRP treatment. The level of activated prorenin in the kidneys of DM + HRP rats was similar to that in the kidneys of C and C + HRP rats (Figure 8, A and C). Because HRP inhibited a nonproteolytic activation of prorenin but did not affect a renin that is proteolytically activated prorenin (Figure 2B), these results suggested that the kidneys of DM rats may have an increased level of nonproteolytically activated prorenin. Although localization of renin in the distal nephron has been reported, we were not able to detect a significant staining by anti-HRP or anti-renin in the tubulointerstitial area in the present study, presumably due to very low level of these nephron segments compared with the juxtaglomerular area that can be seen in the sections.

Discussion

We found that the rat HRP binds to the Abs to the handle region of the prorenin prosegment and inhibits the binding of prorenin to Abs for the anti-handle region (Figure 2A). Moreover, from the studies using Abs to HRP and COS-7 cells expressing rat prorenin receptor protein, we obtained in vitro evidence of prorenin activa-

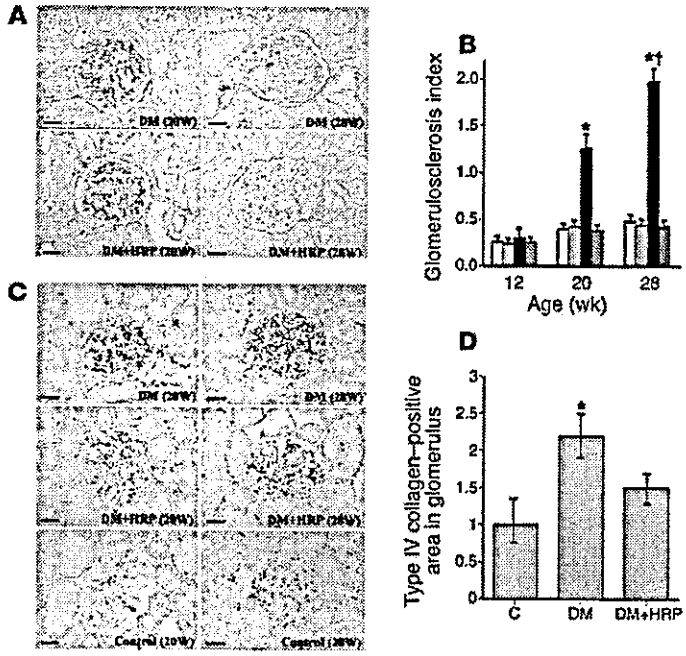

Figure 4
Inhibition of the development of diabetic nephropathy by the HRP of prorenin. (**A**) PAS-stained kidney sections. The photomicrographs show the development and progression of diabetic glomerulosclerosis at 20 weeks of age and later in DM rats. HRP inhibited the development of diabetic glomerulosclerosis in diabetic rats. Scale bars: 50 μm. (**B**) Glomerulosclerosis index of the kidneys in C rats (white bars, $n = 6$), C + HRP rats (light gray bars, $n = 6$), DM rats (black bars, $n = 6$), and DM + HRP rats (dark gray bars, $n = 6$). The graph shows an increase in glomerulosclerosis index at 20 weeks of age and later in DM rats and inhibition of the increase by HRP treatment. $^*P < 0.05$ for DM rats versus the other 3 groups; $^\dagger P < 0.05$ for 28 versus 20 weeks of age. (**C**) Immunohistochemistry of type IV collagen. The photomicrographs show increased glomerular type IV collagen at 20 weeks of age and later in DM rats. HRP inhibited the increase in glomerular type IV collagen in the diabetic rats. Scale bars: 50 μm. (**D**) Quantitative analysis (folds versus C rats) of type IV collagen–positive areas in glomeruli. The graph shows an increase in type IV collagen–positive area in the glomeruli of DM rats at 28 weeks of age and inhibition of the increase by HRP treatment. $^*P < 0.05$ versus C rats.

tion by prorenin receptor or Ab to HRP and inhibition of the activation by HRP. In this mechanism of prorenin activation, we did not see evidence for proteolytic cleavage of prorenin to active renin, suggesting a conformational change as the mechanism. These results support the view that the prorenin elevation in diabetes results in its activation by a nonproteolytic mechanism that is preventable by HRP working as a decoy, which effectively competes for prorenin binding to its receptor inhibiting the proenzyme in activation. Chronic in vivo continuous infusion of HRP by subcutaneous minipumps prevented the increased urinary protein excretion in diabetic rats to levels similar to those of the control rats. HRP did not affect the body weight or blood glucose levels of either control or diabetic rats during 24-week infusion, however, suggesting that HRP did not improve the impaired pancreatic function by the streptozotocin treatment (Figure 3). Also, HRP completely prevented streptozotocin-induced glomerulosclerosis. Also, chronic administration of HRP completely prevented streptozotocin-induced histologically recognizable glomerulosclerosis (Figure 4). These results indicate that the inhibition of nonproteolytic activation of prorenin by HRP completely inhibited the development of nephropathy in rats with streptozotocin-induced diabetes without affecting the hyperglycemic condition.

The ACE inhibitors and Ang II type 1 receptor blockers have significantly attenuated the urinary protein excretion in streptozotocin-induced diabetic rats (10, 11). Prevention of proteinuria and development of glomerulosclerosis in diabetic rats by HRP, however, suggests that HRP may have superior beneficial effects compared with ACE inhibitors or Ang II type 1 receptor blockers. Nguyen et al. recently found that the prorenin/renin receptor(s) is present in the heart, brain, placenta, liver, pancreas, and kidney and activates prorenin by binding proteolysis (9). If HRP competes for prorenin binding to its

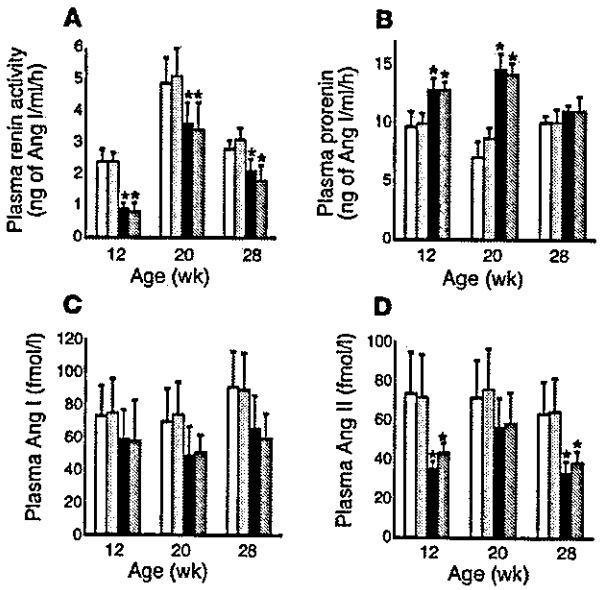

Figure 5
Changes in components of the circulating RAS in C rats (white bars, $n = 6$), C + HRP rats (light gray bars, $n = 6$), DM rats (black bars, $n = 6$), and DM + HRP (dark gray bars, $n = 6$). (**A**) Plasma renin activity. The graph shows decreased plasma renin activity in diabetic rats. HRP did not affect the plasma renin activity of either control or diabetic rats. (**B**) Plasma prorenin concentration. The graph shows increased plasma prorenin concentration in diabetic rats up to 20 weeks of age. HRP did not affect the plasma prorenin concentration of either control or diabetic rats. (**C**) Plasma Ang I concentration. The graph shows a tendency for the plasma Ang I concentration to decrease in diabetic rats. HRP did not affect the plasma Ang I concentration in either control or diabetic rats. (**D**) Plasma Ang II concentration. The graph shows a decreased plasma Ang II concentration in the diabetic rats. HRP did not affect the plasma Ang II concentration in either control or diabetic rats. $^*P < 0.05$ for diabetic versus control rats.

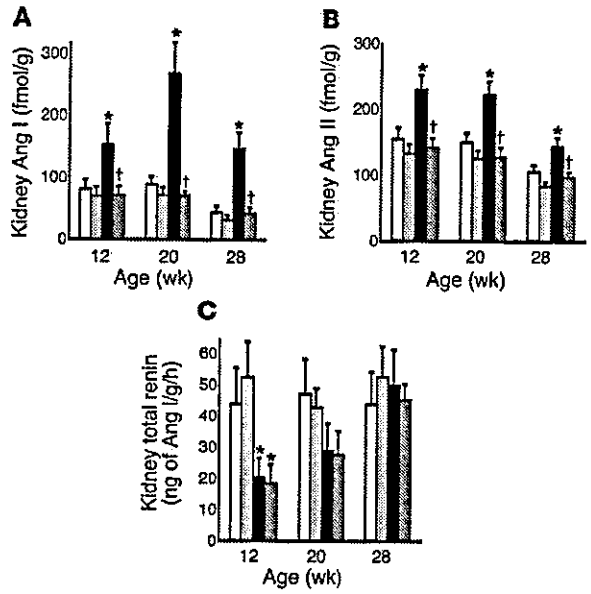

Figure 6
Changes in protein components of the kidney RAS in C rats (white bars, $n = 6$), C + HRP rats (light gray bars, $n = 6$), DM rats (black bars, $n = 6$), and DM + HRP rats (dark gray bars, $n = 6$). (**A**) Kidney Ang I level. The graph shows an increased kidney Ang I level in the DM rats. HRP significantly inhibited the increase in kidney Ang I level in the diabetic rats. (**B**) Kidney Ang II level. The graph shows an increased kidney Ang II level in the DM rats. HRP significantly inhibited the increase in kidney Ang II level in the diabetic rats. (**C**) Kidney total renin level. The graph shows a decreased kidney total renin level in the DM rats at 12 weeks of age. HRP did not affect the kidney total renin level in either control or diabetic rats. $^*P < 0.05$ for DM versus C rats; $^\dagger P < 0.05$ for rats with HRP versus rats without HRP.

receptor resulting in the inhibition of the nonproteolytic activation of prorenin, the complex formation of the prorenin receptor and prorenin may be the major factor in the development of diabetic organ damages. If the complex is also able to activate the ERK1/ERK2 pathways independently of the RAS activation as proposed by Nguyen et al. (9), it is possible that an inhibitor of complex formation between the receptor and prorenin, such as HRP, can completely prevent the development of diabetic organ damages through the inhibition of not only the RAS activation but also the RAS-independent ERK activation.

We measured the RAS components in the plasma of control and diabetic rats (Figure 5). Consistent with previous studies (1, 12), plasma renin activity was significantly lower and plasma prorenin concentration was significantly higher in the DM rats than in the C rats for up to the week 16 of diabetes. The administration of HRP did not affect plasma renin activity or plasma prorenin concentration in either control or the diabetic rats. Although HRP inhibits the interaction between prorenin and its nonproteolytic activators, HRP did not affect the ability of plasma to generate Ang I. The plasma levels of Ang I and II were also lower in the DM rats than in the C rats, and HRP did not influence plasma Ang I or II levels of either control or diabetic rats. In addition, HRP did not affect the BP levels of either control or diabetic rats throughout the 24-week period of HRP infusion. These results suggest that HRP inhibits development of diabetic nephropathy without affecting the circulating RAS or affecting systemic hemodynamics. Since a renin/prorenin receptor, a nonproteolytic activator of prorenin, is exclusively present in tissues but not in circulation (9), HRP may affect tissue RAS but not circulating renin activity or Angs.

There have been conflicting studies showing increased (13), decreased (14), or unchanged (15, 16) kidney Ang II levels in experimental diabetic animals. In these studies, however, kidney Ang II levels were determined at the onset (8 or less weeks) of diabetes without a nephropathy, and to our knowledge, no study had assessed the alterations in the kidney RAS components associated with the development of diabetic nephropathy. In the present study, at 12, 20, and 28 weeks of age (8, 16, and 24 weeks of diabetes), when the diabetic nephropathy developed and progressed, the kidney Ang I and II content of the DM rats markedly increased and was significantly higher than that of the C, C + HRP, and DM + HRP rats (Figure 6, A and B). The kidney Ang I and II content was similar among the C, C + HRP, and DM + HRP rats. The kidney ACE and angiotensinogen mRNA levels were similar in the C, C + HRP, DM, and DM + HRP rats during the 24-week treatment period, consistent with previous studies (17–19) (Figure 7, B and C).

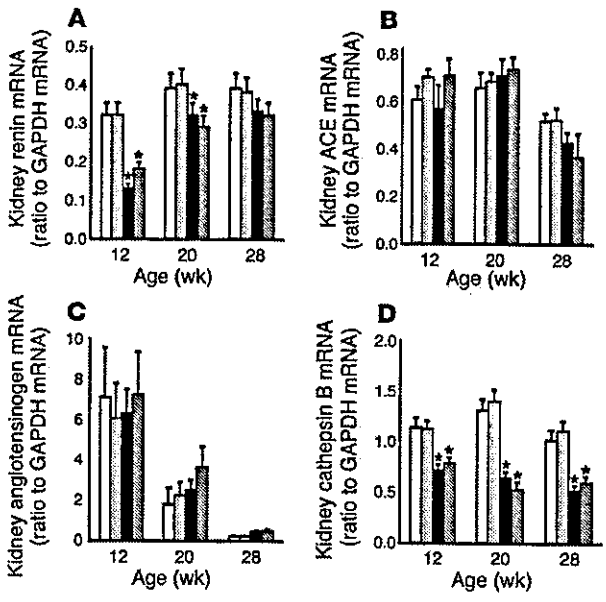

Figure 7
Changes in mRNA components of the kidney RAS in C rats (white bars, $n = 6$), C + HRP rats (light gray bars, $n = 6$), DM rats (black bars, $n = 6$), and DM + HRP rats (dark gray bars, $n = 6$). (**A**) Kidney renin mRNA level. The graph shows a decreased kidney renin mRNA level in the DM rats up to 20 weeks of age. HRP did not affect the kidney renin mRNA level in either control or diabetic rats. (**B**) Kidney ACE mRNA level. The graph shows a decrease in kidney ACE mRNA level at 28 weeks of age in both the control and diabetic rats. HRP did not affect the kidney ACE mRNA level in either control or diabetic rats. (**C**) Kidney angiotensinogen mRNA level. The graph shows a decrease in kidney angiotensinogen mRNA level with age. HRP did not affect the kidney angiotensinogen mRNA level in either control or diabetic rats. (**D**) Kidney cathepsin B mRNA level. The graph shows a decreased kidney cathepsin B mRNA level in the DM rats. HRP did not affect the kidney cathepsin B mRNA level in either control or diabetic rats. $^*P < 0.05$ for diabetic versus control rats.